TMAO Counteracts Urea Denaturation via Urea-Depletion from the Protein Surface

Pritam Ganguly[1], Pablo Boserman[2], Nico F. A. van der Vegt[3], and Joan-Emma Shea*[1,2]

[1]*Department of Chemistry and Biochemistry, University of California at Santa Barbara, Santa Barbara, California 93106, USA.*

[2]*Department of Physics, University of California at Santa Barbara, Santa Barbara, California 93106, USA.*

[3]*Eduard-Zintl-Institut für Anorganische und Physikalische Chemie and Center of Smart Interfaces, Technische Universität Darmstadt, Alarich-Weiss-Straße 10, Darmstadt 64287, Germany.*

Abstract

Osmolytes are small organic molecules that can modulate the stability and function of cellular proteins by altering the chemical environment of the cell. Some of these osmolytes work in conjunction, via mechanisms that are poorly understood. An example is the naturally-occurring protein-protective osmolyte trimethylamine N-oxide (TMAO) that stabilizes cellular proteins in marine organisms against the detrimental denaturing effects of another naturally occurring osmolyte, urea. From a computational standpoint, our understanding of this counteraction mechanism is hampered by the fact that existing force fields fail to capture the correct balance of TMAO and urea interactions in ternary solutions. Using molecular dynamics simulations and Kirkwood-Buff theory of solutions, we have developed an optimized force field that reproduces experimental Kirkwood-Buff integrals. We show through the study of two model systems, a 15-residue polyalanine chain and the R2-fragment (^{273}GKVQIINKKLDL^{284}) of the Tau protein, that TMAO can counteract the denaturing effects of urea by inhibiting protein-urea preferential interaction. The extent to which counteraction can occur is seen to depend heavily on the amino acid composition of the peptide.

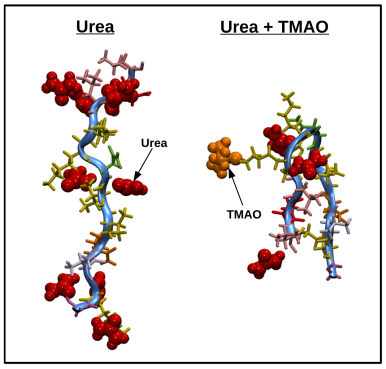

1 INTRODUCTION

In many living organisms, especially in marine animals such as cartilaginous fishes, rays and sharks, urea-induced protein denaturation is counteracted by the naturally occurring protective osmolyte trimethylamine N-oxide (TMAO).[1,2] Much effort has been invested in the last decade into understanding the individual actions of urea and of TMAO on protein structure. The mechanism of urea-induced denaturation has been extensively studied both theoretically and computationally, and it is now accepted that urea acts via a direct mechanism, binding to the protein backbone and side-chains, with little disturbance to water structure.[3–9] Although it is a well-known fact that TMAO stabilizes proteins at pH greater than its own pK_a,[10,11] the mechanism by which TMAO stabilizes proteins in aqueous solutions is perhaps more debated. Many recent experimental and computational studies suggest that TMAO forms a complex with two to three water molecules[12] and that protein stabilization is a result of depletion effects associated with unfavorable interaction of TMAO with the protein backbone[3,13–16] or from the destabilization of the unfolded state by crowding effects.[17] Conversely, it has been suggested that TMAO interacts favorably with polypeptides and that stabilization is a result of a surfactant-like effect of TMAO.[18,19] The counteracting effect of TMAO on urea remains even more controversial.[12,20–24] It has been argued that TMAO decreases the protein solubility by modifying the urea and water structure around the protein which leads to protein-compaction.[21,25–27] Contrarily it has also been argued that TMAO does not modify urea structure around protein.[28,29] It has been shown that the urea-induced unfolding transitions of proteins in terms of the m-values and the protein-urea preferential interactions are unaffected in presence of TMAO[3,30–32] and that TMAO's unfavorable electrostatic interactions with the protein backbone overcome urea's favorable van der Waals interactions with the protein, leading to its compaction.[28] Solvent excluded-volume effects[33] and alteration of protein surface solvation[34] have also been argued to contribute in the counteraction mechanism of TMAO in presence of urea.

In this work, we use computer simulations to shed light into how TMAO counteracts the effects of urea. This approach presents an invaluable tool to probe the combined mechanism of urea/TMAO mixtures on protein structure, as it allows direct observation of the atomistic interactions at play.[25,27–29,35–39] Computational studies of proteins in urea/TMAO/water solutions are however hampered by the fact that urea and TMAO force fields have been parameterized only in binary solutions. In the case of binary urea-water mixtures, the

*Corresponding author. E-mail: shea@chem.ucsb.edu

Smith force field[40] has been parameterized to reproduce experimental thermodynamic quantities related to solvation such as activity coefficients or osmotic coefficients. In the case of binary TMAO-water mixtures, most existing force fields are derived from the *ab initio* based force field developed by Kast and co-workers (the Kast force field[41]). These include the recently developed Usui force field,[42] the density-based double-resolution force field for TMAO-water mixtures (the Shea force field)[43] and the Netz,[44] the García,[15] and the Hölzl force fields.[45] The García force field was parameterized to capture the correct osmotic pressure of TMAO, while the Netz force field reproduces solution activity data and the m-values for glycine, valine, asparagine and the anomaly of tryptophan. The Hölzl model was developed to reproduce experimental solution density and the variation of the activity coefficient. A detailed comparison of the TMAO force-fields, in terms of their hydration and osmotic properties, can be found in the work by Rodríguez-Ropero *et al.*[46] Overall, the most recent TMAO force fields yield satisfactory results when extended to the study of protein folding and aggregation in mixed TMAO/water solutions.[15,47,48] There are however no force fields that have been developed specifically for aqueous solutions of mixed urea and TMAO in order to capture the correct behavior of the solutions in terms of the solvation thermodynamics. Simulations of mixed urea/TMAO systems have simply combined existing urea and TMAO force fields.

In recent work, in an effort to gain insight into how well current TMAO force fields perform in conjunction with the Smith urea force field, we performed molecular dynamics simulations on individual amino acids in mixed aqueous urea/TMAO solutions using five different TMAO force fields (Kast, Netz, Shea, García and Hölzl).[36,49] Our results suggested that the choice of force field had little impact on the outcome of the simulations, with an apparent force field independent mechanism emerging by which urea and TMAO mutually depleted each other from the protein surface. Subsequent work on the association of a small hydrophobic moiety, neopentane, revealed a more complex picture, in which the choice of force field led to significantly different association behavior. Two extreme behaviors were found in the case of the Kast and the Netz force fields. In an earlier simulation work it has been shown that urea causes neopentane association through bridging interactions.[50] Addition of TMAO to the aqueous urea neopentane solution led to complete dissociation of the hydrophobic moieties in the case of the Kast force field, while association was maintained for the Netz force field. Probing deeper, it became apparent that a lower water-affinity and a higher urea-affinity of the Kast TMAO model result into urea-depletion from the neopentane surface which subsequently reduces the neopentane-aggregation by effectively breaking the urea-bridges between the hydrophobic pairs. In contrast, a higher water-affinity of the Netz model was shown to dehydrate urea and neopentane molecules which led to accumulation of urea around the neopentane molecules leading to an increase in their hydrophobic association. Our results showed that a delicate balance between the TMAO-water and the TMAO-urea interactions governs the effects of the urea-TMAO mixtures on hydrophobicity. Clearly, the balance between TMAO/Water/Urea needs to be properly addressed if one wishes to understand the stability of proteins in mixed solutions.

In the present paper, we reparameterize the TMAO/Urea/water ternary solutions using experimentally available data[51] related to solvation thermodynamics to develop a new force field with the proper balance of interactions between the three molecules. We then apply the new force field to the study of polyalanine, a model intrinsically disordered peptide (IDP), and contrast the results to simulations using the unmodified force field. Next, we study the conformational changes of the biologically relevant R2 fragment (^{273}GKVQIINKKLDL^{284}) of the intrinsically disordered Tau protein in pure and mixed urea-TMAO solutions and the preferential interactions of the peptide with the osmolytes. Through the study of these two IDPs we successfully demonstrate how TMAO counteracts urea-denaturations and identify the most important interactions which control the protein-protective properties of TMAO in presence of urea.

2 METHODS

All the molecular dynamics simulations were carried out using the GROMACS molecular dynamics package (version 4.6 and 5.0).[52] The technical details of the simulations are given below.

2.1 Force Fields. Polyalanine was simulated using GROMOS54a7[53] parameters with the rigid SPC/E model for water.[54] The R2 peptide was simulated with the OPLS-AA force field[55–57] combined with the rigid TIP3P water model.[58] For urea the Kirkwood-Buff derived Smith force field was used.[40] TMAO was simulated with the Netz,[44] the Hölzl[45] and the Kast models.[41] The combination rules for the cross-interactions (van der Waals) were as follows: $\sigma_{ij} = \sqrt{\sigma_i \sigma_j}$, $\epsilon_{ij} = \sqrt{\epsilon_i \epsilon_j}$. The non-bonded parameters for these TMAO models are described below.

Along with these TMAO models a newly developed force field for the urea-TMAO solutions was also used. The newly developed force field Netz(m) primarily used the Netz force field for TMAO and the Smith force field for urea with scaled van der Waals parameters for the urea-TMAO and the TMAO-TMAO interactions. For the Netz(m) force field, the cross-interaction terms for the urea-TMAO interactions were $\sigma_{ij} = \sqrt{\sigma_i \sigma_j}$, $\epsilon_{ij} = 1.10 \times \sqrt{\epsilon_i \epsilon_j}$ and for the TMAO-TMAO interactions were $\sigma_{ij} = \sqrt{\sigma_i \sigma_j}$, $\epsilon_{ij} = 0.90 \times \sqrt{\epsilon_i \epsilon_j}$. All the other interaction parameters were according to the original Netz and the Smith force fields. The Kirkwood-Buff integrals (KBIs) for the ternary urea-TMAO-water system at 2 M urea with 1 M TMAO were calculated with both SPC/E and TIP3P water models. It must be noted that unlike constant pH simulations,[83] the protonation states of TMAO have not been considered in this study since the pH of the systems (7.0) is much higher than the pK_a of TMAO (4.6).[30]

2.2 System Details for Polyalanine Simulations and KBI calculations. Cubic simulation boxes with linear dimension of ≈ 5.9 nm were simulated (≈ 5.8 nm for the simulation of polyalanine in pure water). The numbers of osmolyte and water molecules were varied according to the desired Molar concentrations and are

Force field	Atom	σ (nm)	ϵ (kJ mol^{-1})	q (e)
Kast	C	0.3041	0.2826	-0.260
	H	0.1775	0.0773	0.110
	O	0.3266	0.6379	-0.650
	N	0.2926	0.8360	0.440
Netz	C	0.3600	0.2826	-0.260
	H	0.2101	0.0773	0.110
	O	0.3266	0.6379	-0.910
	N	0.2926	0.8360	0.700
Hölzl	C	0.3707	0.2830	-0.260
	H	0.2130	0.0775	0.110
	O	0.3266	0.6389	-0.815
	N	0.2926	0.8374	0.605

Table 1: Non-bonded interaction parameters of the atoms of a TMAO molecule for a) Kast model,[41] b) Netz model,[44] and c) Hölzl model.[45]

System	N_{Urea}	N_{TMAO}	N_{Water}
Water	0	0	6334
1M TMAO	0	125	6265
4M TMAO	0	500	5000
2M Urea	250	0	6000
4M Urea	500	0	5330
6M Urea	750	0	4660
1M Urea + 1M TMAO	125	125	5935
2M Urea + 1M TMAO	250	125	5600
4M Urea + 2M TMAO	500	250	4530
6M Urea + 3M TMAO	750	375	3460
6M Urea + 6M TMAO	750	750	2100

Table 2: The numbers of the molecules for each of the polyalanine simulations and KBI calculations.

system	N_{Urea}	N_{TMAO}	N_{Water}
2M TMAO	0	300	7030
4.1M Urea + 2M TMAO	600	300	5430

Table 3: The numbers of the molecules for the R2 simulations.

listed below. The simulation boxes contained one peptide chain for the polyalanine simulations. The polyalanine chain was uncapped and simulated with neutral termini NH_2 and COOH. A randomly generated helical structure was used as the initial configuration for the chain. For the calculations of the KBIs for the ternary urea-TMAO-water systems (without the polyalanine chain) the same numbers of the osmolytes and the water molecules were used.

2.3 System Details for R2 Simulations. Cubic simulation boxes with linear dimension of ≈ 6.3 nm for R2 in 2 M TMAO and ≈ 6.25 nm for R2 in the mixture of 4.1 M urea and 2 M TMAO were simulated. The simulation boxes contained one R2 peptide in its natural charged state (+2) and two chloride ions were added to neutralize the systems. The N and the C termini of the R2 peptide were capped with the acetyl and the amide groups respectively in order to represent the peptide condition in the context of the full-length Tau protein. A fully extended conformation was used as the initial configuration for the peptide.

2.4 KBI Calculations for Ternary Urea-TMAO-water Mixtures. The KBIs between solution components i and j were calculated from the radial distribution functions $g_{ij}(r)$ between the respective components. The corresponding KBIs (G_{ij}) are defined as,

$$G_{ij} = 4\pi \int_0^\infty \left[g_{ij}(r) - 1\right] r^2 dr. \quad (1)$$

To calculate the KBIs 55 ns NpT simulations of the ternary urea-TMAO-water mixtures were carried out at 300 K temperature and 1 bar pressure with the periodic boundary conditions in the x, y and z directions. For the first 5 ns simulation the Berendsen thermostat (relaxation time 0.5 ps) and barostat[59] (relaxation time 3 ps) were used to maintain the system temperature and pressure respectively. For the next 50 ns simulation the Nosé-Hoover thermostat[60,61] (relaxation time 0.5 ps) and the Parrinello-Rahman barostat[62] (relaxation time 3 ps) were used. A leap-frog integrator was used to integrate the equations of motion with a time step of 2 fs.[63] The particle mesh Ewald (PME) method was used to calculate the electrostatic interactions with a grid-spacing of 0.12 nm.[64] A cut-off of 1.2 nm was used for all the non-bonded interactions. The water molecules were kept rigid by using the SETTLE algorithm.[65] All the bond-distances of the other molecules were kept fixed by using the LINCS algorithm.[66] The same technical parameters were used for all the other simulations (see below) unless mentioned otherwise. The KBIs were calculated from the last 45 ns simulation by taking the average of the running KBIs between 1.0 and 1.4 nm.[67]

2.5 Osmotic Pressure Calculations for Ternary Urea-TMAO-water Mixtures. The osmotic pressure of the systems was calculated using the method proposed by Roux *et al.*[68] To calculate the osmotic pressure of the systems the outputs from the first 5 ns simulations of the KBI calculations (with the Berendsen thermostat and barostat) were used as the initial configurations. These configurations had converged temperatures of 300 K and converged box-volumes corresponding to 1 bar pressure. Let's assume that these converged boxes had x, y and z dimensions as d, d and d. Next these boxes containing urea, TMAO and water were placed at the center of a box with the same x and y dimensions but 2 times the z-dimension (d, d and 2d). The empty spaces of the new box were filled by randomly inserted water molecules. The z-components of the distances of the osmolyte molecules from the center of the box were constrained such a way that the osmolyte molecules were acted upon a restoring force $F(\Delta z) = -k.\Delta z$ towards the center of the box when $|D_z| = \frac{d}{2} + \Delta z$ where D_z is the z-component of the distances of the osmolyte molecules from the center of the box and k is the force-constant. The water molecules were not constrained. Such a way two virtual walls were placed at $z = \pm\frac{d}{2}$ (if we assume that the origin is at the center of the box) which are not permeable for the osmolytes but transparent for the water molecules. The forces on the osmolytes due to these virtual walls were calculated using PLUMED software[69] in conjunction with GROMACS. The bias functions in PLUMED ("UWALLS" and "LWALLS") were modified to calculate the total force on the virtual walls due to the osmolytes instead of calculating the sum of the squared forces on the virtual walls exerted by the individual osmolyte molecule. The distances of the osmolyte molecules from the center of the box were calculated by inserting a non-interacting heavy virtual atom at the center and using the "DISTANCE" function between the virtual heavy atom and the nitrogen atom of TMAO or the carbon atom of urea. The value of the force-constant k (4180 kJ $mol^{-1}nm^{-2}$) was taken from the earlier work by Canchi *et al.*[15] The pressure of the system was constrained at 1 bar only along the z-direction using Parrinello-Rahman barostat with 3 ps relaxation time. The temperature of the system was kept fixed at 300 K using Nosé-Hoover thermostat (relaxation time 0.5 ps). The osmotic pressures of the systems were calculated from the average forces exerted on the virtual walls (same as exerted on the osmolytes) per unit area, which were calculated from 40 ns simulations preceded by 10 ns of equilibrations.

2.6 Replica-exchange Molecular Dynamics Simulations. The replica-exchange molecular dynamics simulations (REMD)[70–72] were performed in NVT ensemble using 64 replicas with temperatures ranging from 291.2 K to 488.9 K. The converged volumes of the systems were obtained from 5 ns NpT simulations at 300 K temperature and and 1 bar pressure using Berendsen thermostat and barostat. These 5 ns NpT simulations were followed by an energy minimization and a 5 ns long NVT simulation at 300 K temperature using Nosé-Hoover thermostat. Then the systems were heated at 64 different temperatures (corresponding to each of the replicas listed below) and were equilibrated for another 5 ns. Then short 5 ns REMDs were performed with 3 ps exchange frequency to check the average probabilities of the replica exchanges. Next with the same exchange

frequency the 150 ns long REMDs for the systems of polyalanine in osmolytes were performed (120 ns for the polyalanine in pure water system) where the last 100 ns simulations were used for the data analyses. For the systems of R2 in 2 M TMAO and in the mixture of 4.1 M urea and 2 M TMAO REMD simulations of 200 and 250 ns were performed respectively where the last 100 ns and 150 ns long trajectories were used for the data analyses respectively. The average exchange probabilities for all the polyalanine systems were $\approx 28\%$ and for the R2 systems were $\approx 25\%$. The corresponding maximum standard deviation in the exchange probabilities for all the replicas was $<2\%$. The temperatures corresponding to the 64 replicas were: 291.2, 293.4, 295.6, 297.8, 300.0, 302.3, 304.6, 306.9, 309.2, 311.6, 314.0, 316.4, 318.9, 321.4, 323.9, 326.5, 329.1, 331.7, 334.4, 337.1, 339.8, 342.6, 345.4, 348.2, 351.1, 354.0, 356.9, 359.9, 362.9, 365.9, 369.0, 372.1, 375.2, 378.4, 381.6, 384.8, 388.1, 391.4, 394.7, 398.1, 401.5, 404.9, 408.4, 411.9, 415.4, 419.0, 422.6, 426.2, 429.9, 433.6, 437.3, 441.1, 444.9, 448.7, 452.6, 456.5, 460.4, 464.4, 468.4, 472.4, 476.5, 480.6, 484.7 and 488.9 K.

2.7 Preferential Solvation Calculations. In a mixture of solute (protein, denoted by p), solvent (water, denoted by w) and cosolvent (urea/TMAO, denoted by c) the preferential solvation/binding coefficient between the solute and the cosolvent can be given as $\Gamma_{\rm pc} = \rho_c(G_{\rm pc} - G_{\rm pw})$ where $G_{\rm ij}$ is the KBI between i and j component. $\Gamma_{\rm pc}$ is a measure of the excess (or deficit) of the cosolvents around the solute molecules with respect to the bulk solvent. Preferential binding coefficients are related to the m-values used in protein denaturation studies.[73–75] The preferential solvation coefficients were calculated from the unnormalized radial distribution functions between the proteins and the solvent components (osmolytes and water) with respect to the surfaces of the proteins and the centers of mass of the solvent components using the following equation:

$$\Gamma_{\rm pc}({\rm r}) = {\rm N_{pc}(r)} - \frac{\rho_{\rm c}}{\rho_{\rm w}}{\rm N_{pw}(r)}, \qquad (2)$$

where $\rm N_{pc}(r)$ and $\rm N_{pw}(r)$ are the running coordination numbers of the cosolvent and the solvent molecules around the protein, respectively, and the ρ-s are the average number densities of the respective components of the solution. For a system with protein (p) in water (w) and two cosolvents, urea (u) and TMAO (t), the preferential solvation coefficient of the protein with urea over TMAO can be given as,

$$\Gamma^{\rm t}_{\rm pu}({\rm r}) = {\rm N_{pu}(r)} - \frac{\rho_{\rm u}}{\rho_{\rm t}}{\rm N_{pt}(r)}, \qquad (3)$$

where $\rm N_{pu}(r)$ and $\rm N_{pt}(r)$ are the running coordination numbers of the urea and the TMAO molecules around protein, respectively. Since the average box-size of the simulations ($\approx 6{\rm nm}$) was much larger than the typical correlation length of the systems ($\approx 1-2\,{\rm nm}$), corrections to the preferential solvation coefficients due to the finite size of the systems were not included.

2.8 Cluster Analyses. Cluster analyses of the protein conformations were performed using the Daura algorithm.[76] Root mean square deviations (RMSD) of the structures were calculated using the positions of the $\rm C_\alpha - C - N$ atoms. Similar structures were grouped together based on their RMSD with a cut-off of 0.2 nm. Respective snapshots were rendered using Visual Molecular Dynamics (VMD) software.[77]

2.9 Hydrogen Bonds and Salt-bridge Analyses for R2 Peptide. The intramolecular hydrogen bonds for the R2 peptide were identified using a cut-off of 0.25 nm for the O–H distances along with a cut-off of 30° for the OHN angles. The salt-bridges between the aspartic acid (D) and the lysine (K) residues were calculated from the distance-distribution between the $\rm COO^-$ and the $\rm NH_3^+$ groups of the sidechains of the respective residues. The salt-bridges were identified when the distance between these two groups was less than the respective cut-off distances. The cut-off distances corresponded to the first minima of the aforementioned distance-distribution curves and were 0.50 nm, 0.51 nm and 0.71 nm for the D283-K274, D283-K280 and D283-K281 salt-bridges respectively. Finally, the probabilities of finding the salt-bridges with respect to the total simulation time were calculated.

2.10 Extraction of Experimental KBI Data (by Rösgen and Jackson-Atogi) In an earlier paper Rösgen and Jackson-Atogi had reported the experimental KBIs for ternary urea-TMAO-water mixtures.[51] In Figure 3 of the aforementioned paper the authors had plotted urea-urea, urea-TMAO, TMAO-TMAO, urea-water, TMAO-water and water-water KBIs for varying TMAO (0 to 2 Molar) and urea (0 to 3.6 molal) concentrations. Although the data corresponding to 2 Molar urea ($\approx$ 2.4 molal, estimated from our simulations) with 1 Molar TMAO were not available, we used three data sets of the plot to efficiently estimate the KBIs at 2 M urea with 1 M TMAO solution and the data sets corresponded to 2.4 molal, 2.0 molal and 1.6 molal urea. The highest concentrations of TMAO corresponding to those data sets were 0.74 Molar, 0.95 Molar and 1.16 Molar respectively. Hence we extrapolated the data corresponding to 2.4 molal and 2.0 molal urea to 1 Molar TMAO concentration and also directly extracted the data corresponding to 1.6 molal urea and 1.0 Molar TMAO. For all the KBIs, the standard deviations of the data obtained from these three data sets were within the line-thickness of the graphs, except for the urea-urea KBIs. Also from the visual inspection of the plot it can be found that for 1 Molar TMAO concentration the urea-dependent offsets of the KBIs are practically indistinguishable from the adjacent curves (except for the urea-urea KBIs). Hence in this paper we reported the data obtained from the extrapolations of the 2.4 molal urea-curves to 1.0 Molar TMAO concentrations as the experimental targets for the development of the urea-TMAO force field. The experimental urea-urea ($\rm G_{uu}$) and TMAO-TMAO ($\rm G_{tt}$) KBIs in urea-TMAO mixtures for 1.6 molal, 2.0 molal and 2.4 molal urea concentrations and the corresponding extrapolations are shown in Figure S1 in the Supporting Information. Please note that the unit of all the experimental data was converted from $L\ mol^{-1}$ to nm^3.

3 RESULTS AND DISCUSSION

3.1 A New Force Field for Ternary Urea/TMAO/water Mixtures. We begin by assessing to which extent simply combining existing urea and TMAO force fields can reproduce experimentally available thermodynamic quantities for ternary urea/TMAO/water solutions. In particular, we focus on osmotic pressure and the Kirkwood-Buff integrals (KBIs) of mixed urea-TMAO solutions that have been experimentally reported by Rösgen and Jackson-Atogi.[51] The KBIs are the volume integrals of the pair correlation functions between the solution components which relate to experimentally observable thermodynamic quantities such as activity derivative, compressibility and partial molar volumes though the Kirkwood-Buff theory of solutions.[78,79] Figure 1 shows the osmolyte-aggregation in terms of the urea-urea, urea-TMAO and TMAO-TMAO KBIs at 2M:1M urea:TMAO concentration. For TMAO we have used three previously reported force fields: the Netz,[44] the Kast,[41] and the Hölzl.[45] When compared to the experimental data

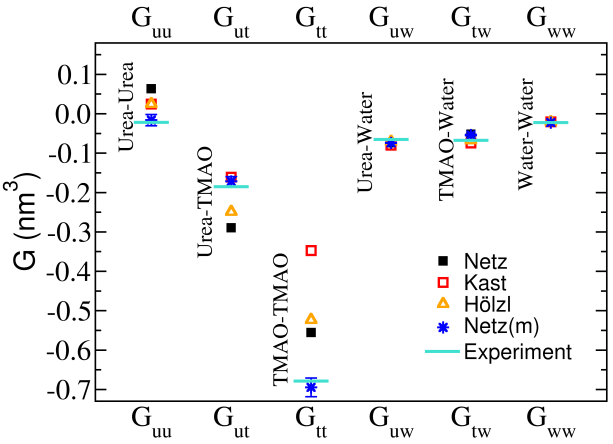

Figure 1: Shown are the urea-urea, urea-TMAO, TMAO-TMAO, urea-water, TMAO-water and water-water Kirkwood-Buff integrals for ternary urea-TMAO-water solution at 2 M urea and 1 M TMAO concentration. The data are obtained using the Kast, the Netz and the Hölzl force fields for TMAO and compared with the results obtained with the newly developed Netz(m) force field for urea-TMAO mixtures. The experimental results are recalculated from the data reported by Rösgen *et al.*[51] through suitable extrapolations.

(using suitable extrapolations, see the methods section for details) the simulation results show a higher urea-urea KBI, a lower urea-TMAO KBI (except with the Kast TMAO model) and a significantly higher TMAO-TMAO self-aggregation. Interestingly, the KBI data related to the hydration of the osmolytes do not show much deviations from experiment. Too high urea-urea and TMAO-TMAO KBIs are clear indications of an over-all high self-aggregations of the osmolytes which is also followed by a lower urea-TMAO aggregation (for the Netz and the Hölzl models). A very high TMAO-TMAO KBI is a signature of the Kast TMAO force field as reported earlier for binary TMAO-water mixture. However, in binary TMAO-water mixtures, the Netz and the Hölzl models reproduce solution activity and so does the Smith urea model for binary urea-water mixtures. Hence any deficiencies in the urea and the TMAO models in predicting osmolyte-aggregation correctly in mixed urea-TMAO mixture must arise from the incorrect interactions between these molecules, and necessitate the reparameterization of the force fields, particularly with a focus on the osmolyte-osmolyte interactions.

Having identified the interactions that are incorrectly captured by simply mixing urea and TMAO, we can now proceed to reparameterize the interactions so as to reproduce experimental KBIs of the solution components of a urea-TMAO mixture. We validate our force field developments on the basis of the experimental KBI data for ternary urea-TMAO water solutions at 2 M urea with 1 M TMAO concentration. As mentioned in the previous paragraph, the urea-TMAO force fields discussed so far yield high urea-urea and TMAO-TMAO KBIs and low urea-TMAO KBIs compared to the experiments. For the Netz TMAO force field in particular, a very low urea-TMAO KBI is noted.

Based on this observation, we modify the urea-TMAO force fields (the Smith urea force field and the Netz and the Hölzl TMAO force fields) by first increasing the effective interactions between urea and TMAO to reproduce the experimental KBIs for the ternary urea-TMAO-water systems at 2M:1M urea-TMAO concentration. At this point we refrain ourselves from modifying any other interactions in the systems such as the hydration propensities of the osmolytes because the urea (the Smith) and the TMAO force fields (the Netz and the Hölzl) show correct variations in the solution activity for binary urea-water and TMAO-water solutions respectively and also the hydration data for the mixed urea-TMAO solution match well with the experiments (Figure 1). We gradually increase the urea-TMAO van der Waals interactions with a scaling factor ranging from 1.0 (no scaling) to 1.5 and calculate the KBIs between the solution components for the ternary urea-TMAO-water systems at 2 M urea and 1 M TMAO concentration.

However, as seen from the relevant KBIs for the ternary urea-TMAO-water systems (see Figure S2 in the Supporting Information), we find that using this single scaling factor does not yield satisfactory results. Scaling factors ($\geq$1.2) result into high urea-TMAO KBIs. Conversely a low scaling-factor ($<$1.2) cannot correct for the TMAO-TMAO KBIs and predict very high values for it. It is clear that the corrections for all three urea-urea, urea-TMAO and TMAO-TMAO KBIs cannot sufficiently be met through solely modifying urea-TMAO interactions. Rather, it must be met through the proper balance between all the individual osmolyte aggregations, that is, through properly balancing urea-urea, urea-TMAO, and TMAO-TMAO aggregations. Hence we scale down the van der Waals interactions between the TMAO molecules (to correct for the overly high TMAO-TMAO aggregation obtained by just mixing the urea and TMAO force fields), along with scaling up the urea-TMAO interactions. For this we scale down the TMAO-TMAO van der Waals interactions with a factor ranging from 1.0 (unscaled) to 0.8 for different values of the scaling factor for the urea-TMAO interactions. Using the Netz force field for TMAO we find that the scaling factors of 0.9 for the TMAO-TMAO and 1.1 for the urea-TMAO van der Waals interactions yield the best over-all match with all the experimental urea-urea, urea-TMAO, TMAO-TMAO, urea-water, TMAO-water and water-water KBIs. Henceforth in this paper the newly developed force field for urea-TMAO mixtures is termed as the Netz(m) force field. Relevant KBI data obtained with the Netz(m) force field for the mixture of 2 M urea with 1 M TMAO are shown in Figure 1. To develop the final version of the urea-TMAO force field we have chosen the Netz force field over the Hölzl force field because the Netz force field has been tested for predicting the m-value of polyglycine in TMAO-water correctly[44] whereas the suitability of the Hölzl model to study protein-TMAO interactions has not been tested previously. We have further applied the Netz(m) model to calculate the relevant KBIs at a different osmolyte concentration (1 M urea with 1 M TMAO) and an extremely good overall agreement with the experimental results has been found, except for a slightly high urea-TMAO KBI (Figure S3 in the Supporting Information). Experimental KBIs[51] show very little to practically no dependency on the urea concentration (for a fixed TMAO concentration) which is reasonably well captured by the Netz(m) force field. All the calculations discussed above used rigid SPC/E water model.[54] In Figure S4 in the Supporting Information we also show the KBI data for 2 M urea and 1 M TMAO using Netz(m) model with TIP3P water model[58] and the results compare reasonably well with the experiments except for a moderately high urea-TMAO KBI. Along with the KBIs we have also calculated the osmotic pressure of the urea-TMAO mixtures (using SPC/E water) at 2 M urea and 1 M TMAO using the methodology proposed by Roux *et al.* (details provided in the methodology section).[68] When compared with the experimental osmotic pressure (78.3 bar)[51] our simulations show slightly higher osmotic pressure of the system. The osmotic pressures obtained with the different TMAO force fields are as follows: Netz 93.3 ± 1.8 bar, Kast 85.3 ± 0.5 bar, Hölzl 90.9 ± 2.0 bar and no significant improvement to the results has been found us-

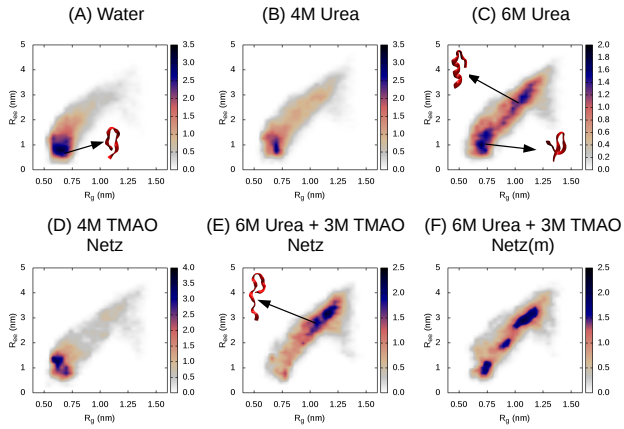

Figure 2: Distributions of the radius of gyration (R_g) and the end-to-end distance (R_{ee}) of a 15 amino acid long polyalanine chain in water and in pure and mixed urea-TMAO solutions. Representative snapshots corresponding to the different conformations of the peptide are also shown. The Netz TMAO force field has been used for the simulations of 4 M TMAO. For the urea-TMAO mixtures the Netz and the Netz(m) force fields have been used as indicated in the figure.

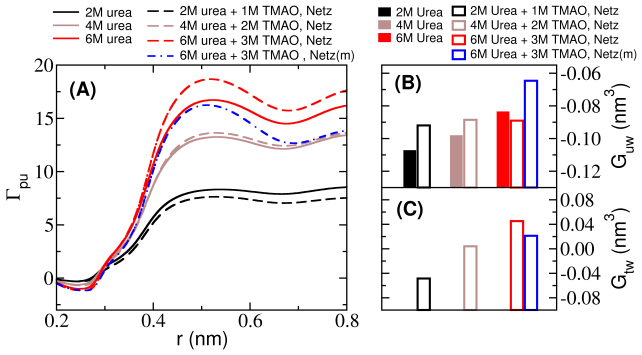

Figure 3: (A) Shown are the preferential solvation coefficients between polyalanine and urea in pure urea solutions with increasing urea concentrations and compared with the results obtained after TMAO added to the systems at 2:1 urea:TMAO concentration ratio. (B) Urea-water KBIs (G_{uw}) for polyalanine in 2 M, 4 M and 6 M urea solutions (solid bars) and compared with the data obtained after TMAO is added at 2:1 urea:TMAO concentration ratio (hollow bars). (C) Corresponding TMAO-water KBIs (G_{tw}) for mixed urea-TMAO solutions containing polyalanine. The results obtained with the Netz TMAO force field and the Netz(m) urea-TMAO force fields are compared (blue dashed line in panel A and blue hollow bars in panel B and C).

ing the Netz(m) force field (89.8 ± 1.0 bar).

We have also calculated the densities of the urea-TMAO solutions with different TMAO [Kast, Netz, Hölzl and Netz(m)] and water models (SPC/E and TIP3P) at 2:1 urea-TMAO concentrations and compared the densities with the experimental values obtained from the data by Rösgen and Jackson-Atogi.[51] The corresponding data (up to 6 M urea with 3 M TMAO) are plotted in the Supporting Information, Figure S5. We have found that the density of the urea-TMAO solution depends both on the water and the TMAO models. The unmodified Netz model combined with the SPC/E water model predicts slightly higher densities at the higher urea-TMAO concentrations (>4 M urea) and the modifications to the urea-TMAO and TMAO-TMAO Lennard-Jones parameters (Netz(m) model) do not have any significant effect on the solution density. However, when the Netz(m) model is combined with TIP3P water the solution densities are reasonably well-reproduced at the higher osmolyte concentrations. The Hölzl model with SPC/E water predicts the correct densities of the urea-TMAO solutions. However, when the Hölzl model is combined with TIP3P water model, it predicts solution densities lower than the experimental ones. From our data it is evident that it is not straightforward to develop urea-TMAO force-fields which would reproduce both the KBIs and the densities. In terms of reproducing KBIs (up to 2 M urea and 1 M TMAO concentration, which is the highest concentration of the osmolytes at 2:1 ratio with experimentally available KBI data) and solution density (up to 6 M urea with 3 M TMAO) we find that the Netz(m) force-field provides the best compromise, even when the effects of different water models are taken into consideration.

3.2 Structure and Preferential Solvation of Polyalanine in Osmolyte Mixtures.

We now turn to the study of a model intrinsically disordered peptide, a 15-residue long polyalanine chain, and investigate its structure in water, urea, TMAO (Netz), and in the uncorrected and corrected (Netz(m)) mixed urea/TMAO force fields. It has been shown experimentally that TMAO counteracts urea's effects at 2:1 to 1:1 urea:TMAO concentration ratios[80–82] and we will therefore focus on these ratios.

Figure 2 shows the distributions of the radius of gyration (R_g) of the polyalanine chain along with its end-to-end distance (R_{ee}) for different solvent conditions. Higher values of R_g and R_{ee} indicate extended structures of the peptide chain and conversely the lower values of R_g and R_{ee} are found in collapsed or compact conformations of the chain. In pure water (without the osmolytes) the chain predominantly assumes a very compact conformation (Figure 2A). Upon addition of urea the chain starts exploring more the extended structures and it starts to sample both the extended and the compact structures with comparable probabilities at 6 M urea (Figure 2C). In contrast, the chain primarily remains in the compact conformations in pure TMAO solutions (using Netz TMAO force field) as seen from the results obtained at 4 M TMAO (Figure 2D). For mixed urea/TMAO solutions with the uncorrected force field (Figure 2E), a 2:1 mixture of 3 M TMAO (Netz) with 6 M urea leads to further unfolding of the polyalanine chain over a pure urea solution. Similar results have been found with the Kast model too (see the Supporting Information, Figure S6). In contrast, from Figure 2(F) we find that the peptide samples both the compact and the extended conformations with comparable probabilities when the newly developed Netz(m) force field for urea-TMAO is used.

The TMAO-induced denaturation with the unmodified urea/TMAO(Netz) force fields can be understood by considering the aggregation propensity of urea around the protein. We plot the preferential solvation coefficient of the peptide with urea (Γ_{pu}) in pure urea solutions with increasing urea concentrations and compare the results with 2:1 urea:TMAO solutions at the same urea concentrations in Figure 3(A). We find that the addition of 1 M TMAO (Netz) to 2 M urea effectively excludes urea molecules from the vicinity of the protein, hence reducing the protein-urea preferential solvation. We note that the preferential interactions include the direct and the solvent-mediated indirect interactions between the solute (peptide) and the solvent molecules (urea, TMAO and water). Consequently, a decrease in the peptide-urea preferential interaction may not necessarily imply a direct-depletion of urea

from the protein surface but it implies an "effective" decrease in the urea density over water density in the vicinity of protein with respect to the bulk urea/water density. Henceforth in this paper the exclusion or the depletion of the urea (or TMAO) molecules from protein will refer to the aforementioned "effective" decrease in the urea (or TMAO) density around protein. As opposed to the lower urea-TMAO concentrations, from Figure 3(A) we find that when TMAO (Netz) is added at the 2:1 urea:TMAO concentration ratio to the urea solutions at high urea concentrations ($\geq$4 M), TMAO tends to promote urea-aggregation around protein. In contrast, when 3 M TMAO is added to 6 M urea system using the Netz(m) force field, the peptide-urea preferential interaction reduces. Figure S7 (upper panel) in the Supporting Information shows the corresponding short-range interaction energy between the peptide and the urea molecules in terms of the Coulomb and the van der Waals interactions and it can be seen that the Netz(m) force field makes the urea-peptide electrostatic interactions unfavorable when 3 M TMAO is added to 6 M urea solutions, whereas the unmodified Netz force field slightly enhances the urea-peptide van der Waals interaction.

From Figure 3(B) it can also be seen that the Netz(m) force field enhances urea-hydration propensity (urea-water KBI) upon addition of TMAO as opposed to the unmodified Netz force field which dehydrates urea molecules. This difference in the modification of the hydration of urea can be correlated with the lower water affinity (TMAO-water KBI) of the TMAO molecules in the Netz(m) model over that of the unmodified Netz TMAO model, as seen from Figure 3(C). It must be noted that in contrast to the simulations performed with the higher osmolyte concentrations, the differences in osmolyte hydration for the Netz and the Netz(m) models are not significant at the lower urea-TMAO concentrations (2 M urea with 1 M TMAO), as seen from the urea-water and the urea-TMAO KBIs (without polyalanine) in Figure 1. Nonetheless, in the case of the higher osmolyte concentrations it can be argued that the Netz(m) force field effectively depletes urea from the peptide and promotes the compaction of the peptide structure by the virtue of a comparatively higher urea-TMAO interaction (by design) and a lower TMAO-water interaction, in contrast to the unmodified Netz force field. It is also very interesting to see that qualitatively the reduction in the peptide-urea preferential solvation does not depend on the peptide conformations. In the Supporting Information (Figure S8) we plot the relevant peptide-urea preferential solvations, separately for the very compact ($R_g < 0.8$ nm) and the very extended ($R_g > 1.0$ nm) structures. We find that upon the addition of 3 M TMAO to 6 M urea the peptide-urea preferential solvation decreases for both the compact and the extended conformations. In addition, we also study the conformational changes of polyalanine and the corresponding peptide-osmolyte preferential interactions at 6M:6M (1:1) urea/TMAO solution. From the relevant plots (Figure S9) in the Supporting Information we find that the population of the compact structures increases with the increase in TMAO concentration which is followed by a significantly larger decrease in protein-urea preferential solvation (see section "Polyalanine in 6 M urea with 6 M TMAO" and Figures S10, S11 and S12 in the Supporting Information for details). A strong correlation between the decrease in the peptide-urea preferential solvation with the increase in the compact peptide conformations has also been found by increasing the urea-TMAO van der Waals interaction (details are given in the Supporting Information, Figures S6, S13 and S14). Thus all the above results clearly point at a mechanism of effective urea-exclusion from the vicinity of protein with the addition of TMAO which potentially contributes to the increased population of the compact conformations of the peptide.

3.3 Counteraction of Urea-denaturation of R2 Peptide by TMAO. We now consider a second IDP peptide, the GKVQIINKKLDL (R2) peptide of the microtubule-binding protein Tau that flanks the R2 repeat of full-length Tau and a linker region containing the highly aggregation prone PHF6* segment VQIINK. In earlier work, we studied the regulation of this peptide in pure TMAO and in pure urea solutions, and showed that R2 peptide maintains compact conformations in TMAO while it samples both the extended and the compact structures in urea solution.[47] Here, as in the case of polyalanine, we study the conformations of this protein in mixed urea/TMAO solutions with the Netz(m) force field. Figure 4(A) shows the relevant distributions of R_g and R_{ee} of the peptide in different solvent conditions. In pure water and in 2 M TMAO the peptide predominantly samples compact conformations ($R_g < 0.8$ nm) while in urea it acquires a broad range of conformations, sampling both the compact and the extended domains with comparable probabilities. The addition of TMAO to urea solution at $\approx$2:1 urea:TMAO ratio dramatically changes the distributions of R_g and R_{ee} with significantly more compact structures (($R_g < 0.8$ nm)) are sampled. The cluster analysis (shown in Figure 4(C)) of the peptide conformations reveals that the most probable conformations in water are well maintained in TMAO solutions but significantly perturbed in urea solution. The addition of TMAO in urea solution retrieves the majority of the most probable conformations corresponding to water or TMAO solutions.

Having demonstrated the counteraction of TMAO against urea-denaturation we study the protein-osmolyte preferential interactions associated with the relative stability and changes of the peptide-conformations. Figure 4(B) plots the preferential solvation coefficients of the peptide with urea ($\Gamma_{\rm pu}$) for urea and mixed urea-TMAO solutions. $\Gamma_{\rm pu}$ for the urea solution has been calculated using the data obtained earlier by Levine *et al.*[47] The addition of TMAO to a comparable concentration of urea (4.1 M) as in the pure urea solution (4.4 M) reduces the protein-urea preferential solvation. Similar to the case of polyalanine, the reduction in the protein-urea preferential solvation is independent of the protein conformations, as seen from Figure S15 in the Supporting Information. The corresponding peptide-urea interaction energies, in terms of the Coulomb and the van der Waals interactions, become unfavorable when TMAO is added to urea solution, as seen from Figure S7 (lower panel) in the Supporting Information. These results strongly suggest that the effective removal of urea from the peptide correlates with the counteraction of urea-denaturation by TMAO. For the R2 peptide, a moderate depletion of the TMAO molecules around peptide by the addition of urea can also be found by comparing the protein-TMAO preferential binding ($\Gamma_{\rm pt}$) for TMAO and mixed urea-TMAO solutions.

Along with solvation properties, intramolecular interactions such as formation of intramolecular hydrogen bonds or salt-bridges in R2 peptide contributes to the formation and the stability of compact structures. To explore how the osmolytic solutions impact the formation of hydrogen bonds and salt-bridges in R2, we plot the probability distributions of the number of intramolecular hydrogen bonds and the probabilities of occurrence of different salt-bridges (between D and K residues) within the R2 peptide in Figure S16 in the Supporting Information for different solvent conditions. The probability of formation of hydrogen bonds (> 4) in R2 (see Figure S16 in the Supporting Information, upper panel) is significantly higher in pure water or 2 M TMAO solution than in 4.4 M urea or in the mixture of 4.1 M urea with 2 M TMAO. The addition of TMAO to water does not perturb the hydrogen-bonding propensity of R2 significantly, similar to our earlier findings.[47] However, it is intriguing to find that the addition of TMAO to urea solution has no significant effect on the intramolecular hydrogen bonds when compared to the urea solu-

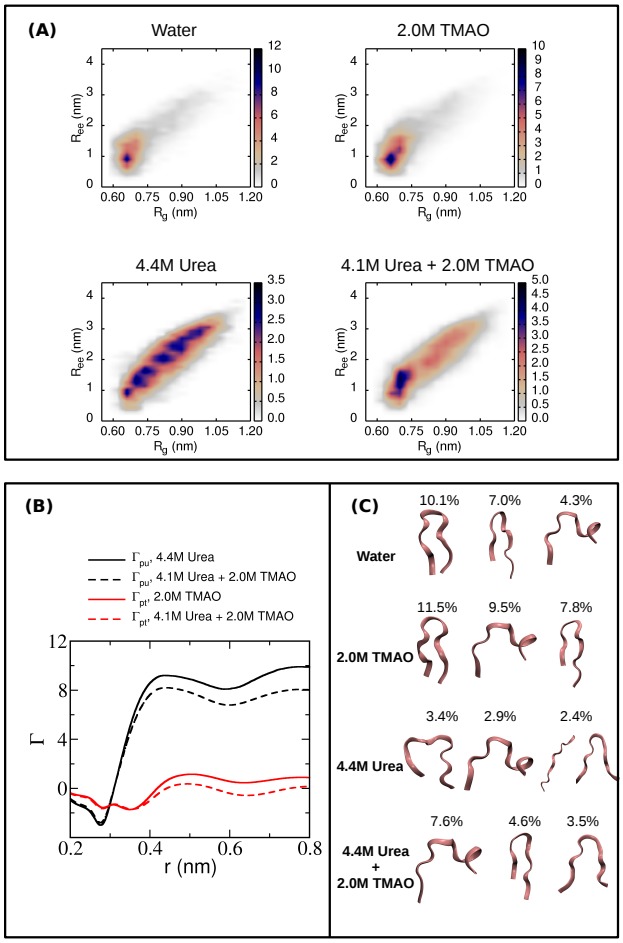

Figure 4: (A) Distributions of the radius of gyration (R_g) and the end-to-end distance (R_{ee}) of the R2 peptide in pure water, 4.4 M urea, 2 M TMAO and in the mixture of 4.1 M urea with 2 M TMAO. The TMAO solution without urea is modeled with the Netz TMAO force field. The urea-TMAO mixture is modeled with the newly developed Netz(m) force field for urea-TMAO. (B) Urea-protein ($\Gamma_{\rm pu}$) and TMAO-protein ($\Gamma_{\rm pt}$) preferential solvation coeffcients for 4.4 M urea, 2 M TMAO and mixed 4.1 M urea with 2 M TMAO solutions. (C) The most probable conformations of the R2 peptide in different solvent conditions. The plots corresponding to 4.4 M urea and pure water are reanalyzed from the data reported earlier by Levine *et al.*[47]

tion, suggesting that TMAO does not counteract urea's effects on the R2 peptide through modification of intramolecular hydrogen-bonding propensity. In contrast, TMAO is found to significantly increase the probability of the formation of the D283-K274 salt-bridge (see Figure S16 in the Supporting Information, lower panel).[47] Similarly, in another recent study involving Trp-cage miniprotein, the addition of TMAO in water has been found to enhance the interaction propensities between the oppositely chraged residues.[84] However in R2, unlike the D283-K274 salt-bridge, the other two salt-bridges (D283-K280 and D283-K281) are found to be destabilized by the addition of TMAO. Despite of the fact that the addition of TMAO to water inhibits the formation of the D283-K280 and the D283-K281 salt-bridges and does not alter the average number of the intramolecular hydrogen bonds, the R2 peptide maintains its compact conformations in TMAO. These results prompt us to infer that in the overall compaction of the peptide, the D283-K274 salt-bridge, formed by two distant residues which are located near the two ends of the peptide, prevails over the other two salt-bridges formed by nearby residues. In urea solution the formation of D283-K274 salt-bridge is significantly suppressed. Interestingly, when TMAO is added to urea solution, the effect of urea on the formation of D283-K274 salt-bridge is compensated and the probability of D283-K274 salt-bridge formation in mixed urea-TMAO solution at 2:1 urea:TMAO ratio is very similar to that found in pure water. Taken as a whole, the results discussed above lead us to a counteraction mechanism by TMAO in presence of urea where an effective removal of urea molecules from the R2 peptide promotes compact conformations of the peptide through the retrieval of D283-K274 salt-bridge.

4 CONCLUSIONS

In this paper we have addressed the biologically important question of how protective osmolytes influence protein stability in the presence of denaturing osmolytes by studying the conformational changes of two model peptides, polyalanine and the R2-fragment of the Tau protein, in pure and mixed TMAO/urea solutions. Using molecular dynamics simulations we have first identified deficiencies in existing urea-TMAO force fields that lead to an incorrect description of the solvation thermodynamics of the urea-TMAO solutions. We introduce a new combined force field for urea-TMAO mixtures that reproduces experimental data related to the solvation thermodynamics of urea-TMAO solutions. Through developing this new force field for urea-TMAO mixtures we have studied how the variations in the osmolyte-osmolyte interactions lead to the conformational changes of polyalanine and identified that the effective removal of urea from the vicinity of the protein by TMAO is strongly correlated with the increased population of the compact conformations of the protein. By studying another model IDP, the R2-fragment of the Tau protein, the counteraction to urea-denaturation is also shown to correlate with the reduction in the peptide-urea preferential solvation when TMAO is added to urea solutions at 2:1 urea:TMAO concentration. Along with effectively depleting urea from R2, TMAO is found to stabilize the peptide through enhancing the propensity of the D283-K274 salt-bridge formation. In contrast, since polyalanine cannot make any salt-bridges, this may explain why the peptide is significantly less structured than R2, in water and in osmolyte solutions, as seen in the probabilities of their most probable conformations. The counteracting effect of TMAO is more pronounced for the case of R2 than for polyalanine which correlates with the presence of relatively more stable compact conformations in R2 peptide than polyalanine, with or without the osmolytes. Addition of TMAO in the urea solution of R2 leads to relatively unfavorable van der Waals and Coulomb energies between the peptide and urea, whereas for the polyalanine systems, only the Coulomb energy component becomes unfavorable without any significant decrease in the peptide-urea van der Waals interactions. Since favorable van der Waals interactions between protein and urea are known to drive urea-denaturation of proteins,[28] this would explain the more effective counteraction of urea by TMAO in the case of R2, although urea-depletion by TMAO is observed in both R2 and polyalanine systems.

ACKNOWLEDGMENTS

This work was supported by the Extreme Science and Engineering Discovery Environment (XSEDE) through National Science Foundation (NSF) grant numbers TG-MCA05S027 and TG-CHE160034. J.-E.S. expresses gratitude for the support from the National Science Foundation (NSF Grant MCB-1716956) and from the Center for Scientific Computing at the California Nanosystems Institute (NSF

Grant CNS-0960316). The computational resources at the Texas Advanced Computing Center at the University of Texas at Austin and the San Diego Super Computing at the University of California, San Diego are greatly acknowledged. We thank Martin Kurnik for many helpful discussions.

SUPPORTING INFORMATION AVAILABLE

The Supporting Information (SI) file contains supplemental figures showing KBIs for the urea-TMAO mixtures, modeled with Netz(m) force field, at 1 M urea with 1 M TMAO (using SPC/E water) and at 2 M urea with 1 M TMAO (using TIP3P water). KBIs for the urea-TMAO mixtures, the distributions of R_g and R_{ee} of polyalanine in urea-TMAO mixtures and the corresponding protein-urea and protein-TMAO preferential solvation coefficients with different scaling factors for the urea-TMAO van der Waals interactions are also shown. The SI contains the distribution of R_g and the four most probable conformations of polyalanine in the mixture of 6 M urea with 6 M TMAO. The preferential solvation coefficients of protein with urea over TMAO are also shown for the mixtures of 6 M urea with 3 M TMAO and 6 M urea with 6 M TMAO. For R2 peptide in urea-TMAO mixtures, the probability distributions of the intramolecular hydrogen bonds and salt-bridges are plotted. The interaction energies between the peptides and urea are plotted for polyalanine and R2 in urea and in urea-TMAO solutions. The experimental urea-urea and TMAO-TMAO KBI data for urea-TMAO mixtures[51] are replotted and the corresponding extrapolations to 1 M TMAO concentration are also shown. The densities of the 2:1 urea-TMAO mixtures are shown for different TMAO and water models and the results are compared with the experiments.

REFERENCES

(1) Yancey, P. H.; Somero, G. N. Counteraction of Urea Destabilization of Protein Structure by Methylamine Osmoregulatory Compounds of Elasmobranch Fishes. *Biochem. J.* **1979**, *183*, 317–323.

(2) Yancey, P. H.; Clark, M. E.; Hand, S. C.; Bowlus, R. D.; Somero, G. N. Living with Water Stress: Evolution of Osmolyte Systems. *Science* **1982**, *217*, 1214–1222.

(3) Wang, A.; Bolen, D. W. A Naturally Occurring Protective System in Urea-Rich Cells: Mechanism of Osmolyte Protection of Proteins against Urea Denaturation. *Biochemistry* **1997**, *36*, 9101–9108.

(4) Auton, M.; Holthauzen, L. M. F.; Bolen, D. W. Anatomy of Energetic Changes Accompanying Urea-induced Protein Denaturation. *Proc. Natl. Acad. Sci. U.S.A.* **2007**, *104*, 15317–15322.

(5) Rossky, P. J. Protein Denaturation by Urea: Slash and Bond. *Proc. Natl. Acad. Sci. U.S.A.* **2008**, *105*, 16825–16826.

(6) Hua, L.; Zhou, R. H.; Thirumalai, D.; Berne, B. J. Urea Denaturation by Stronger Dispersion Interactions with Proteins than Water Implies a 2-stage Unfolding. *Proc. Natl. Acad. Sci. U.S.A.* **2008**, *105*, 16928–16933.

(7) Canchi, D. R.; Paschek, D.; García, A. Equilibrium Study of Protein Denaturation by Urea. *J. Am. Chem. Soc.* **2010**, *132*, 2338–2344.

(8) Guinn, E. J.; Pegram, L. M.; Capp, M. W.; Pollock, M. N.; Record, M. T. Quantifying Why Urea is a Protein Denaturant, Whereas Glycine Betaine is a Protein Stabilizer. *Proc. Natl. Acad. Sci.* **2011**, *108*, 16932–16937.

(9) Moeser, B.; Horinek, D. Unified Description of Urea Denaturation: Backbone and Side Chains Contribute Equally in the Transfer Model. *J. Phys. Chem. B* **2014**, *118*, 107–114.

(10) Singh, R.; Haque, I.; Ahmad, F. Counteracting Osmolyte Trimethylamine N-Oxide Destabilizes Proteins at pH below Its $\mathrm{pK_a}$. *J. Biol. Chem.* **2005**, *280*, 11035–11042.

(11) Foglia, F.; Carullo, P.; Del Vecchio, P. The Effect of Trimethylamine N-oxide on RNase a Stability. *J. Therm. Anal. Calorim.* **2008**, *91*, 67–72.

(12) Hunger, J.; Ottoson, N.; Mazur, K.; Bonn, M.; Bakker, H. J. Water-mediated Interactions Between Trimethylamine-N-oxide and Urea. *Phys. Chem. Chem. Phys.* **2015**, *17*, 298–306.

(13) Rose, G.; Fleming, P.; Banavar, J.; Maritan, A. A Backbone-based Theory of Protein Folding. *Proc. Natl. Acad. Sci. U.S.A.* **2006**, *103*, 16623–16633.

(14) Bolen, D. W.; Rose, G. D. Structure and Energetics of the Hydrogen-Bonded Backbone in Protein Folding. *Annu. Rev. Biochem.* **2008**, *77*, 339–362.

(15) Canchi, D. R.; Jayasimha, P.; Rau, D. C.; Makhatadze, G. I.; García, A. E. Molecular Mechanism for the Preferential Exclusion of TMAO from Protein Surfaces. *J. Phys. Chem. B* **2012**, *116*, 12095–12104.

(16) Canchi, D. R.; García, A. E. Cosolvent Effects on Protein Stability. *Annu. Rev. Phys. Chem.* **2013**, *64*, 273–293.

(17) Cho, S. S.; Reddy, G.; Straub, J. E.; Thirumalai, D. Entropic Stabilization of Proteins by TMAO. *J. Phys. Chem. B* **2011**, *115*, 13401–13407.

(18) Liao, Y.-T.; Manson, A. C.; DeLyser, M. R.; Noid, W. G.; Cremer, P. S. Trimethylamine N-oxide Stabilizes Proteins via a Distinct Mechanism Compared with Betaine and Glycine. *Proc. Natl. Acad. Sci. U.S.A.* **2017**, *114*, 2479–2484.

(19) Mondal, J.; Halverson, D.; Li, I. T. S.; Stirnemann, G.; Walker, G. C.; Berne, B. J. How Osmolytes Influence Hydrophobic Polymer Conformations: A Unified View from Experiment and Theory. *Proc. Natl. Sci. Acad. U. S. A.* **2015**, *112*, 9270–9275.

(20) Rezus, Y. L. A.; Bakker, H. J. Destabilization of the Hydrogen-Bond Structure of Water by the Osmolyte Trimethylamine N-Oxide. *J. Phys. Chem. B* **2009**, *113*, 4038–4044.

(21) Meersman, F.; Bowron, D.; Soper, A. K.; Koch, M. H. Counteraction of Urea by Trimethylamine N-Oxide Is Due to Direct Interaction. *Biophys. J.* **2009**, *97*, 2559–2566.

(22) Meersman, F.; Bowron, D.; Soper, A. K.; Koch, M. H. J. An X-ray and Neutron Scattering Study of the Equilibrium between Trimethylamine N-oxide and Urea in Aqueous Solution. *Phys. Chem. Chem. Phys.* **2011**, *13*, 13765–13771.

(23) Sahle, C. J.; Schroer, M. A.; Juurinen, I.; Niskanen, J. Influence of TMAO and Urea on the Structure of Water Studied by Inelastic X-ray Scattering. *Phys. Chem. Chem. Phys.* **2016**, *18*, 16518–16526.

(24) Ohto, T.; Hunger, J.; Ellen Backus, E.; Mizukami, W.; Bonn, M.; Nagata, Y. Trimethylamin-N-oxide: Hydration Structure, Surface Activity, and Biological Function Viewed by Vibrational Spectroscopies and Molecular Dynamics Simulations. *Phys. Chem. Chem. Phys.* **2017**, DOI: 10.1039/C6CP07284D.

(25) Paul, S.; Patey, G. N. Structure and Interaction in Aqueous Urea-Trimethylamine-N-oxide Solutions. *J. Am. Chem. Soc.* **2007**, *129*, 4476–4482.

(26) Mukaiyama, A.; Koga, Y.; Takano, K.; Kanaya, S. Osmolyte Effect on the Stability and Folding of a Hyperthermophilic Protein. *Proteins* **2008**, *71*, 110–118.

(27) Yang, Y.; Mu, Y.; Li, W. Microscopic Significance of Hydrophobic Residues in the Protein-stabilizing Effect of Trimethylamine N-oxide (TMAO). *Phys. Chem. Chem. Phys.* **2016**, *18*, 22081–22088.

(28) Kokubo, H.; Hu, C. Y.; Pettitt, B. M. Peptide Conformational Preferences in Osmolyte Solutions: Transfer Free Energies of Decaalanine. *J. Am. Chem. Soc.* **2011**, *133*, 1849–1858.

(29) Smolin, N.; Voloshin, V.; Anikeenko, A.; Geiger, A.; Winter, R.; Medvedev, N. N. TMAO and Urea in the Hydration Shell of the Protein SNase. *Phys. Chem. Chem. Phys.* **2017**, *19*, 6345–6357.

(30) Lin, T. Y.; Timasheff, S. N. Why Do Some Organisms Use a Urea-methylamine Mixture as Osmolyte? Thermodynamic Compensation of Urea and Trimethylamine N-oxide Interactions with Protein. *Biochemistry* **1994**, *33*, 12695–12701.

(31) Mello, C.; Barrick, D. Measuring the Stability of Partly Folded Proteins Using TMAO. *Protein Sci.* **2003**, *12*, 1522–1529.

(32) Holthauzen, L. M. F.; Bolen, D. W. Mixed Osmolytes: The Degree to Which One Osmolyte Affects the Protein Stabilizing Ability of Another. *Protein Sci.* **2007**, *16*, 293–298.

(33) Graziano, G. How does Trimethylamine N-oxide Counteract the Denaturing Activity of Urea? *Phys. Chem. Chem. Phys.* **2011**, *13*, 17689–17695.

(34) Rösgen, J. Synergy in ProteinOsmolyte Mixtures. *J. Phys. Chem. B* **2015**, *119*, 150–157.

(35) Bennion, B. J.; Daggett, V. Counteraction of Urea-induced Protein Denaturation by Trimethylamine N-oxide: A Chemical Chaperone at Atomic Resolution. *Proc. Natl. Acad. Sci. U.S.A.* **2004**, *101*, 6433–6438.

(36) Ganguly, P.; Hajari, T.; Shea, J.-E.; van der Vegt, N. F. A. Mutual Exclusion of Urea and Trimethylamine N-oxide from Amino Acids in Mixed Solvent Environment. *J. Phys. Chem. Lett.* **2015**, *6*, 581–585.

(37) Sarma, R.; Paul, S. Exploring the Molecular Mechanism of Trimethylamine-N-oxide's Ability to Counteract the Protein Denaturing Effects of Urea. *J. Phys. Chem. B* **2013**, *117*, 5691–5704.

(38) Borgohain, G.; Paul, S. Model Dependency of TMAO's Counteracting Effect Against Action of Urea: Kast Model versus Osmotic Model of TMAO. *J. Phys. Chem. B* **2016**, *120*, 2352–2361.

(39) Borgohain, G.; Paul, S. Effect of Nonpolar Confinement on Protein Trp cage Conformation in Aqueous Osmolyte Solutions. *J. Mol. Liq.* **2017**, *231*, 174–184.

(40) Weerasinghe, S.; Smith, P. E. A Kirkwood-Buff Derived Force Field for Mixtures of Urea and Water. *J. Phys. Chem. B* **2003**, *107*, 3891–3898.

(41) Kast, K. M.; Brickmann, J.; Kast, S. M.; Berry, R. S. Binary Phases of Aliphatic N-Oxides and Water: Force Field Development and Molecular Dynamics Simulation. *J. Phys. Chem. A* **2003**, *107*, 5342–5351.

(42) Usui, K.; Nagata, Y.; Hunger, J.; Bonn, M.; Sulpizi, M. A New Force Field Including Charge Directionality for TMAO in Aqueous Solution. *J. Chem. Phys.* **2016**, *145*, 064103.

(43) Larini, L.; Shea, J.-E. Double Resolution Model for Studying TMAO/Water Effective Interactions. *J. Phys. Chem. B* **2013**, *117*, 13268–13277.

(44) Schneck, E.; Horinek, D.; Netz, R. R. Insight into the Molecular Mechanisms of Protein Stabilizing Osmolytes from Global Force-field Variations. *J. Phys. Chem. B* **2013**, *117*, 8310–8321.

(45) Hölzl, C.; Kibies, P.; Imoto, S.; Frach, R.; Suladze, S.; Winter, R.; Marx, D.; Horinek, D.; Kast, S. M. Design Principles for High–pressure Force Fields: Aqueous TMAO Solutions from Ambient to Kilobar Pressures. *J. Chem. Phys.* **2016**, *144*, 144104.

(46) Rodríguez-Ropero, F.; Rötzscher, P.; van der Vegt, N. F. A. Comparison of Different TMAO Force Fields and Their Impact on the Folding Equilibrium of a Hydrophobic Polymer. *J. Phys. Chem. B* **2016**, *120*, 8757–8767.

(47) Levine, Z. A.; Larini, L.; LaPointe, N. E.; Feinstein, S. C.; Shea, J.-E. Regulation and Aggregation of Intrinsically Disordered Peptides. *Proc. Natl. Acad. Sci. U.S.A.* **2015**, *112*, 2758–2763.

(48) Muttathukattil, A. N.; Reddy, G. Osmolyte Effects on the Growth of Amyloid Fibrils. *J. Phys. Chem. B* **2016**, *120*, 10979–10989.

(49) Ganguly, P.; van der Vegt, N. F. A.; Shea, J.-E. Hydrophobic Association in Mixed UreaTMAO Solutions. *J. Phys. Chem. Lett.* **2016**, *7*, 3052–3059.

(50) Lee, M.-E.; van der Vegt, N. F. A. Does Urea Denature Hydrophobic Interactions? *J. Am. Chem. Soc.* **2006**, *128*, 4948–4949.

(51) Rösgen, J.; Jackson-Atogi, R. Volume Exclusion and H-Bonding Dominate the Thermodynamics and Solvation of Trimethylamine-N-oxide in Aqueous Urea. *J. Am. Chem. Soc.* **2012**, *134*, 3590–3597.

(52) Hess, B.; Kutzner, C.; van der Spoel, D.; Lindahl, E. GROMACS 4: Algorithms for Highly Efficient, Load-Balanced, and Scalable Molecular Simulation. *J. Chem. Theory Comput.* **2008**, *4*, 435–447.

(53) Schmid, N.; Eichenberger, A. P.; Choutko, A.; Riniker, S.; Winger, M.; Mark, A. E.; van Gunsteren, W. F. Definition and Testing of the GROMOS Force-field Versions 54A7 and 54B7. *Eur. Biophys. J.* **2011**, *40*, 843–856.

(54) Berendsen, H. J. C.; Grigera, J. R.; Straatsma, T. P. The Missing Term in Effective Pair Potentials. *J. Phys. Chem.* **1987**, *91*, 6269–6271.

(55) Jorgensen, W. L.; Maxwell, D. S.; Tirado-Rives, J. Development and Testing of the OPLS All-Atom Force Field on Conformational Energetics and Properties of Organic Liquids. *J. Am. Chem. Soc.* **1996**, *118*, 11225–11236.

(56) Rizzo, R. C.; Jorgensen, W. L. OPLS All-Atom Model for Amines: Resolution of the Amine Hydration Problem. *J. Am. Chem. Soc.* **1999**, *121*, 4827–4836.

(57) Kaminski, G. A.; Friesner, R.; Tirado-Rives, J.; Jorgensen, W. L.; Evaluation and Reparametrization of the OPLS-AA Force Field for Proteins via Comparison with Accurate Quantum Chemical Calculations on Peptides. *J. Phys. Chem. B* **2001**, *105*, 6474–6487.

(58) Jorgensen, W. L.; Chandrasekhar, J.; Madura, J. D.; Impey, R. W.; Klein, M. L. Comparison of Simple Potential Functions for Simulating Liquid Water. *J. Chem. Phys.* **1983**, *79*, 926.

(59) Berendsen, H. J. C.; Postma, J. P. M.; van Gunsteren, W. F.; DiNola, A.; Haak, J. R. Molecular Dynamics with Coupling to an External Bath. *J. Chem. Phys.* **1984**, *81*, 3684–3690.

(60) Nosé, S. A Molecular Dynamics Method for Simulations in the Canonical Ensemble. *Mol. Phys.* **1984**, *52*, 255–268.

(61) Hoover, W. G. Canonical Dynamics: Equilibrium Phase-space Distributions. *Phys. Rev. A* **1985**, *31*, 1695.

(62) Parrinello, M.; Rahman, A. Polymorphic Transitions in Single Crystals: A New Molecular Dynamics Method. *J. Appl. Phys.* **1981**, *52*, 7182.

(63) Verlet, L. Computer "Experiments" on Classical Fluids. I. Thermodynamical Properties of Lennard-Jones Molecules. *Phys. Rev.* **1967**, *159*, 98.
(64) Essmann U.; Perera L.; Berkowitz M. L.; Darden T.; Lee H.; Pedersen L. G. A Smooth Particle Mesh Ewald Method. *J. Chem. Phys.* **1995**, *103*, 8577–8593.
(65) Miyamoto, S.; Kollman, P. A. Settle: An Analytical Version of the SHAKE and RATTLE Algorithm for Rigid Water Models. *J. Comput. Chem.* **1992**, *13*, 952–962.
(66) Hess, B.; Bekker, H.; Berendsen, H. J. C.; Fraaije, J. G. E. M. LINCS: A Linear Constraint Solver for Molecular Simulations. *J. Comput. Chem.* **1997**, *18*, 1463–1472.
(67) Ganguly, P.; van der Vegt, N. F. A. Convergence of Sampling Kirkwood-Buff Integrals of Aqueous Solutions with Molecular Dynamics Simulations. *J. Chem. Theory Comput.* **2013**, *9*, 1347–1355.
(68) Luo Y.; Roux B. Simulation of Osmotic Pressure in Concentrated Aqueous Salt Solutions. *J. Phys. Chem. Lett.* **2010**, *1*, 183–189.
(69) Tribello, G. A.; Bonomi, M.; Branduardi, D.; Camilloni, C.; Bussi, G. PLUMED2: New Feathers for an Old Bird. *Comp. Phys. Comm* **2014**, *185*, 604–613.
(70) Hukushima, K.; Nemoto, K. Exchange Monte Carlo Method and Application to Spin Glass Simulations. *J. Phys. Soc. Jpn.* **1996**, *65*, 1604–1608.
(71) Sugita, Y.; Okamoto, Y. Replica-exchange Molecular Dynamics Method for Protein Folding. *Chem. Phys. Lett.* **1999**, *314*, 141–151.
(72) Patriksson, A.; van der Spoel, D. A Temperature Predictor for Parallel Tempering Simulations. *Phys. Chem. Chem. Phys.* **2008**, *10*, 2073–2077.
(73) Wyman Jr., J. Linked Functions and Reciprocal Effects in Hemoglobin: A Second Look. *Adv. Protein Chem.* **1964**, *19*, 223–286.
(74) Tanford, C. Extension of the Theory of Linked Functions to Incorporate the Effects of Protein Hydration. *J. Mol. Biol.* **1969**, *39*, 539–544.
(75) Timasheff, S. N. Protein-solvent Preferential Interactions, Protein Hydration, and the Modulation of Biochemical Reactions by Solvent Components. *Proc. Natl. Acad. Sci. U.S.A.* **2002**, *99*, 9721–9726.
(76) Daura, X.; Gademann, K.; Jaun, B.; Seebach, D.; van Gunsteren, W. F.; Mark, A. E. Peptide Folding: When Simulation Meets Experiment. *Angew. Chem., Int. Ed.* **1999**, *38*, 236–240.
(77) Humphrey, W.; Dalke, A.; Schulten, K. VMD–Visual Molecular Dynamics. *J. Molec. Graphics* **1996**, *14*, 33–38.
(78) Kirkwood, J. G.; Buff, F. P. The Statistical Mechanical Theory of Solutions. I. *J. Chem. Phys.* **1951**, *19*, 774.
(79) Ben-Naim, A. *Molecular Theory of Solutions*; Oxford University Press: New York, 2006.
(80) Yancey, P. H.; Somero, G. N. Methylamine Osmoregulatory Solutes of Elasmobranch Fishes Counteract Urea Inhibition of Enzymes. *J. Exp. Zool.* **1980**, *212*, 205–213.
(81) Palmer, H. R.; Bedford, J. J.; Leader, J. P.; Smith, R. A. J. ^{3}1P and ^{1}H NMR Studies of the Effect of the Counteracting Osmolyte Trimethylamine-N-oxide on Interactions of Urea with Ribonuclease A. *J. Biol. Chem.* **2000**, *275*, 27708–27711.
(82) Gluick, T. C.; Yadav, S. Trimethylamine N-Oxide Stabilizes RNA Tertiary Structure and Attenuates the Denaturating Effects of Urea. *J. Am. Chem. Soc.* **2003**, *125*, 4418–4419.
(83) Denning, E. J.; Thirumalai, D.; MacKerell Jr., A. D. Protonation of Trimethylamine N-oxide (TMAO) is Required for Stabilization of RNA Tertiary Structure. *Biophys. Chem.* **2013**, *184*, 8–16.
(84) Su, Z.; Mahmoudinobar, F.; Dias, C. L. Effects of Trimethylamine-N-oxide on the Conformation of Peptides and its Implications for Proteins. *Phys. Rev. Lett.* **2017**, *119*, 108102.